SERDs: A Case Study in Targeted Protein Degradation

Journal:	*Chemical Society Reviews*
Manuscript ID	CS-REV-02-2022-000117.R1
Article Type:	Tutorial Review
Date Submitted by the Author:	15-Jul-2022
Complete List of Authors:	Wang, Lucia; Stevens Institute of Technology, Chemistry and Chemical Biology Sharma, Abhishek; Stevens Institute of Technology,

SCHOLARONE™
Manuscripts

ARTICLE

SERDs: A Case Study in Targeted Protein Degradation

Lucia Wang and Abhishek Sharma[*]

Endocrine therapies for breast cancer target ERα which is found in more than 70% of breast cancers. Unfortunately, endocrine resistance typically occurs, in which case Selective Estrogen Receptor Degraders (SERDs) represent the last line of treatment for metastatic breast cancer patients. Fulvestrant, the only currently approved SERD and one of the first targeted protein degradation therapies, presents poor drug-like properties which has led to the development of a new generation of oral SERDs. This review summarizes recent progress in the evolution of SERDs, focusing on clinical candidates and their degradation motifs within the broader context of targeted protein degradation therapies.

Key learning points

(1) Current challenges in the treatment of Estrogen Receptor-α positive breast cancer

(2) Fundamental structural design of antiestrogens

(3) Role of the ubiquitin-proteasome system in SERD-induced degradation

(4) Analysis of degradation motifs in the search for orally bioavailable SERDs

(5) Promising future directions and challenges in the design of next-generation therapies

---

1. Introduction

Breast cancer remains the most common cancer among women, accounting for approximately 25% of new cases and 16% of cancer mortality worldwide.[1] Breast cancer is a highly heterogeneous disease, characterized by different immunohistochemical biomarkers, risk factors, clinical outcome and response to treatment.[2] Of the clinical molecular subtypes, 70-80% are Estrogen Receptor alpha (ERα)-positive and are dependent on ERα signaling for tumor growth and progression.[3] Endocrine therapies represent the standard-of-care treatment for early-stage ERα-positive breast cancer and act by inhibiting estrogen biosynthesis (e.g. aromatase inhibitors, AIs)[4] or competitive binding to ERα (e.g. Selective ER Modulators, SERMs).[5] However, long-term treatment with the pioneer SERM tamoxifen (**1**, Figure 1) is known to promote endometrial cancer and thromboembolic disease due to its partial ERα agonism.[6] Second generation SERMs, including raloxifene (**3**) and lasofoxifene (**4**), present decreased uterotrophic activity but none have been proved to be effective in advanced disease.[7] In addition, disease recurrence and resistance typically occur in as many as 30-50% of patients, restricting the use of the above-mentioned agents and posing a significant challenge for optimal clinical management of advanced metastatic breast cancer

patients.[8] Multiple molecular mechanisms are known to contribute to therapeutic resistance, including ligand-independent activation via PI3K-AKT-mTOR and RAS/RAF/MEK/ERK pathways[9] as well as *ESR1* gain-of-function mutations (Y537S, D538G)[10] in the gene region encoding the ligand binding domain of the receptor. Based on the previous observations, high-affinity ERα ligands that fully antagonize and target ERα for proteasome-dependent degradation have been proposed to overcome tamoxifen/AI refractory disease.[11]

Lucia Wang received her BPharm degree from the University San Pablo CEU (Spain). She then joined Stevens Institute of Technology where she is currently a PhD student in Chemical Biology under the supervision of Dr. Abhishek Sharma. Her research focuses on the design and synthesis of new antiestrogens for the treatment of breast cancer.
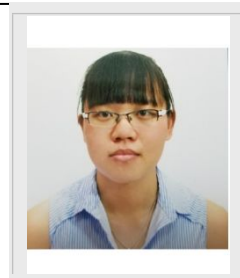
Department of Chemistry and Chemical Biology
Stevens Institute of Technology
Hoboken, New Jersey 07030 (USA)
E-mail: abhishek.sharma@stevens.edu

Selective Estrogen Receptor Degraders (SERDs) offer the ability to not only antagonize ERα but also downregulate ERα protein levels. These molecules represent one of the earliest examples of targeted protein degradation therapeutics. Fulvestrant (**5**, Figure 1) is the first and only clinically approved SERD, showing efficacy in tamoxifen-refractory patients and postmenopausal women with *ESR1* mutations who had progressed on prior aromatase inhibitors.[12] However, Fulvestrant has multiple pharmacokinetic limitations that hamper its widespread use and clinical efficacy. Because of Its low aqueous solubility, it is administered as an intramuscular injection.[13] The current approved loading-dose regimen (500 mg dose on days 1, 15 and 29) improved *in vivo* exposure and progression-free survival, compared with the AI anastrozole (**2**, Figure 1), but steady-state plasma concentrations take months to establish and residual ERα expression remains detectable in *in vitro* experiments.[14, 15] Moreover, the distribution and metabolism of Fulvestrant are significantly limited by its high degree of binding to plasma proteins (99%) and extensive metabolism *in vivo*.[16] Therefore, there is a compelling medical need for potent orally bioavailable SERDs that could reach steady-state free drug levels more rapidly, leading to faster clinical responses, and achieve complete receptor knockdown. Here, we briefly review recent progress in the design and development of SERDs, with special emphasis on those that have progressed into clinical trials over the past few years and their degradation motifs.
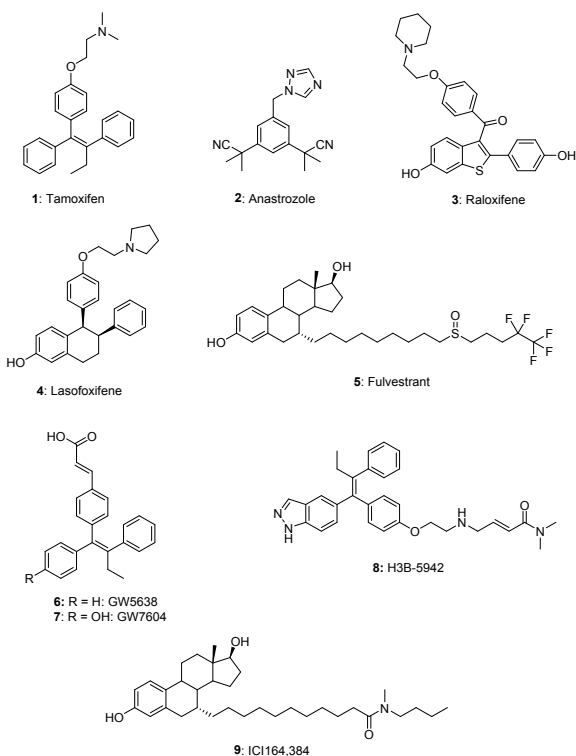

Figure 1. Chemical structures of SERMs (**1, 3, 4**), AIs (**2**), SERDs (**5-7, 9**) and SERCAs (**8**).

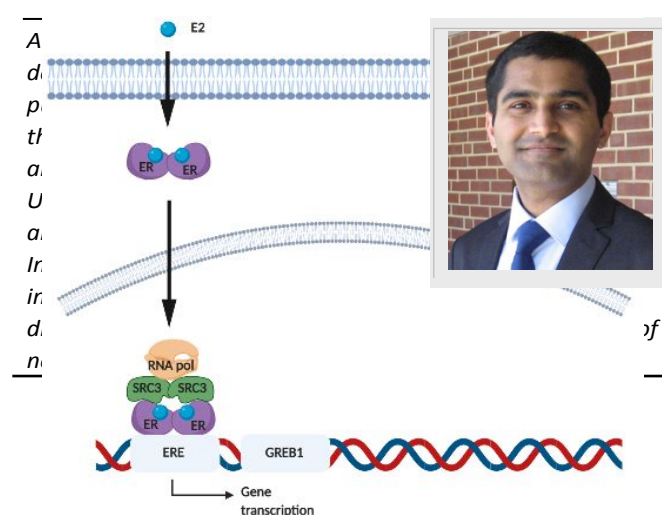## 2. Mechanism of action of SERDs

2.1. ERα conformational changes

Figure 2. ERα signaling pathway. Estradiol (E2) diffuses across the plasma membrane and binds to cytosolic ERα, causing receptor dimerization and translocation to nucleus. The ERα dimer binds to specific DNA promoter sequences (estrogen response elements, ERE) activating downstream gene transcription. This process is dependent on recruitment of coactivator peptides (SRC3) and RNA polymerase.

ERα is a member of the nuclear receptor superfamily of proteins that act as transcription factors.[17] The receptor is not a molecular on/off switch but rather presents a highly plastic pharmacology, where its overall conformation is determined by the nature of the bound ligand. In particular, helix-12 (h12) of the ligand binding domain (LBD) is highly dynamic and allows the formation of protein-protein interaction surfaces with coregulator peptides of the SRC family of proteins. Following estradiol (E2) binding, h12 is aligned over the ligand binding cavity and converts the activating function 2 (AF-2) domain into a hydrophobic groove able to recruit coactivator peptides with the conserved LXXLL sequence motif.[18] This active ERα conformation causes its nuclear translocation and binding to DNA promoter regions known as estrogen response elements (EREs), activating the transcription of downstream target genes (Figure 2). On the other hand, antiestrogens sterically interfere with h12 and maintain the LBD in an "open" conformation which is no longer suitable for coactivator recruitment, but instead accessible to corepressors.[19]

The molecular design of antiestrogens (Figure 3) consists of a phenolic core which mimics the Glu353/Arg394 hydrogen bond network found in the E2-ERα complex. This core serves as anchor for different side chains, the nature of which determines the overall ERα conformation. Selective ER Modulators (SERMs) bear a positively charged basic side chain that forms an ionic interaction with Asp351, displacing h12 and blocking further coactivator binding, while Selective ER Degraders (SERDs) increase the exposed hydrophobic surface and target the receptor for ubiquitination and proteasomal degradation.[20] Furthermore, Fulvestrant and GW5638 (**6**) cause ERα downregulation through different protein conformations. The long alkyl side chain of Fulvestrant protrudes out of the ligand binding pocket (Figure 4A) and directly blocks the coactivator binding groove[21] whereas the acrylate carboxyl group of GW5638 establishes a hydrogen bond with Asp351 (Figure 4B)
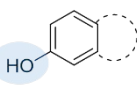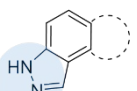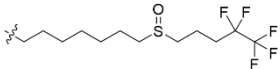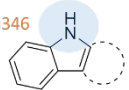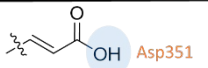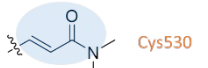
Figure 3. Molecular design of ERα antagonists, consisting of various side chains attached to a central ERα ligand core. Functionalities highlighted in blue indicate chemical groups involved in key binding interactions with ERα protein residues (labeled in orange).

and partially displaces h12 from its interaction site within the coactivator binding cleft.[22] More recently, a new class of ERα antagonists termed as Selective ER Covalent Antagonists (SERCAs) was disclosed.[23] H3B-5942 (**8**) has an acrylamide moiety which acts as a Michael acceptor and reacts with a nonconserved cysteine residue (C530) located at the end of helix-11. The gain of potency through such covalent interaction inactivates both wild-type and *ESR1* mutant ERα.

2.2. Role of the ubiquitin-proteasome system

The ubiquitin-proteasome system (UPS) constitutes the main protein degradation machinery along with autophagy-lysosomal pathway. The mechanisms of ubiquitin-dependent protein degradation were revealed through pioneering biochemical studies from Aaron Ciechanover, Avram Hershko and Irwin Rose,[24–26] culminating in the award of the 2004 Nobel Prize in Chemistry. This system comprises a cascade of enzymes (Figure 5) that activate (E1 activating enzyme), conjugate (E2 conjugating enzyme) and ligate (E3 ligase) ubiquitin molecules to lysine residues on the surface of the target protein. Initially, ubiquitin is activated in an ATP-dependent step, resulting in formation of a high-energy thioester bond with a cysteine residue within the active site of the E1 activating enzyme. Subsequently, ubiquitin is trans-thiolated to the E2 conjugating enzyme active-site cysteine and the E3 ligase facilitates the transfer of ubiquitin from the E2-Ub intermediate to the substrate protein. E3 ligases exert a special role within this cascade as they bring the substrate and E2-Ub intermediate in close spatial proximity forming a ternary complex which simultaneously enhances the rate of ubiquitin transfer. Ubiquitin contains several lysine residues itself which undergo ubiquitination as well, forming polyubiquitinated chains which direct the conjugated protein to the 26S proteasome for ATP-dependent proteolysis.

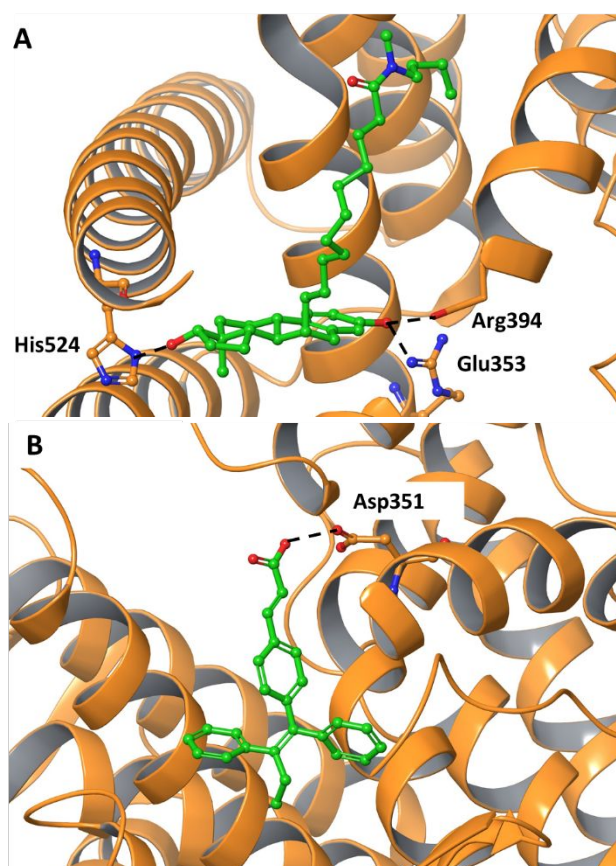Cellular levels of ERα are tightly regulated by distinct degradation pathways that converge on the ubiquitin-26S

Figure 4. A) Key binding interactions of ICI164,384 **9** (an analog of fulvestrant **3**, PDB code 1HJ1) within the ERα ligand binding pocket (orange ribbon). The long side chain of ICI164,384 **9** (green carbon atoms) exits the ligand binding pocket and blocks h12 repositioning over the coactivator binding groove. B) The acrylate functionality of GW5638 **6** (PDB code 1SRK) forms a hydrogen bond with Asp351.

proteasome system and are differentially affected by the nature of the bound ligand.[20] In the absence of E2, apo-ERα is degraded by dynamic interactions with heat-shock proteins (including Hsp90), cochaperones and the ubiquitin ligase CHIP, resulting in a half-life of 4-5 h.[27, 28] Specifically, lysine residues K302 and K303, located in the hinge-region, play a key role in regulating receptor polyubiquitination and subsequent turnover.[29] Estradiol binding accelerates receptor degradation in a typical hormone-dependent negative feedback loop, reducing its half-life to 3-4 h due to a transcription-coupled degradation pathway requiring new protein synthesis.[27] However, inhibition of 26S proteasomal activity prevents but does not entirely inhibit E2-induced degradation.[30] This observation suggests the presence of other cellular proteolytic mechanisms that regulate receptor abundance and cell proliferation, including lysosomal and autophagy pathways.[30, 31]

Time course experiments showed that ERα protein levels decreased by 60% and 80% after 1 h and 4 h of E2 treatment, respectively.[32] After 16 h, protein levels are restored and equivalent to the ones observed 1 h after addition of E2. In contrast, treatment with Fulvestrant caused 95% ERα turnover after 1 h exposure. The observed higher degradation rate is related to the greater degree of protein ubiquitination.[20] Interestingly, the extent to which the GW7604-ERα complex is ubiquitinated is not significantly different from basal levels,
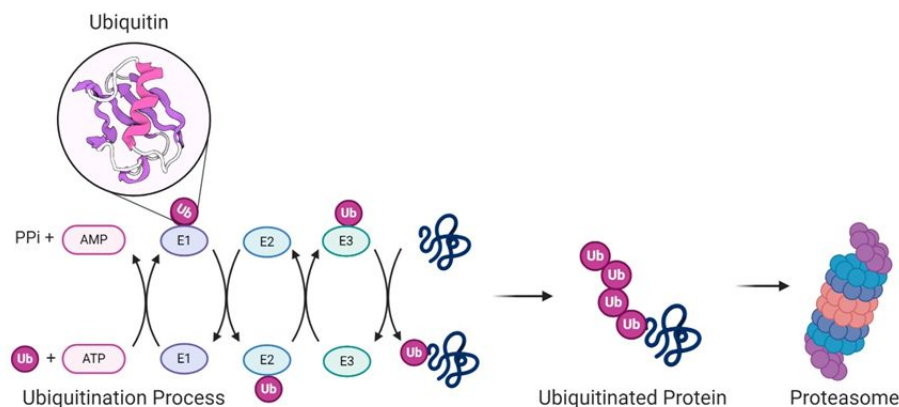
Figure 5. Overview of the ubiquitin/proteasome system (UPS). Initially, ubiquitin is activated in an ATP-dependent step, resulting in formation of a high-energy thioester bond with a cysteine residue within the active site of the E1 activating enzyme. Subsequently, ubiquitin is trans-thiolated to the E2 conjugating enzyme active-site cysteine and the E3 ligase facilitates the transfer of ubiquitin from the E2-Ub intermediate to the substrate protein.

suggesting that the mechanisms leading to GW7604- and Fulvestrant-induced degradation are uncoupled and that other factors besides ubiquitination may affect the rate at which ERα is degraded. However, ERα downregulation and transcriptional activity do not have a direct correlation. The decrease in ERα protein levels is more pronounced after treatment with SERDs than after addition of E2, while E2 and SERDs have a comparable effect on *ESR1* mRNA transcription levels. [20]

3. Trends in SERD development

3.1. Phenol bioisosteres

The earliest efforts to synthesize orally bioavailable SERDs consisted of Fulvestrant analogs where the long alkyl chain at the 7α position of the estrogen core was modified to increase its aqueous solubility.[33, 34] Although the resulting compounds were more effective than tamoxifen or Fulvestrant at degrading ERα and inhibiting the growth of human breast cancer xenografts, serum concentrations did not increase at 4-24 h after injection compared to Fulvestrant.[33] This observation could be explained by the fact that these studies did not address the metabolic soft spots arising from the common phenol group, which is known to undergo rapid and extensive *O*-glucuronidation and *O*-sulfation to form inactive phase II metabolites.[35] In 2016, Liu and co-workers reported a boronic acid analog[36] (ZB716 **10,** Figure 6) of Fulvestrant which exhibited similar SERD and antiproliferative potencies while demonstrating enhanced oral bioavailability. In 2017, the same group applied this phenol-boronic acid bioisosterism to the acrylic acid-based SERD GW7604 (**7**, Figure 6), resulting in compound GLL398 **11**.[37] The boronate derivative had a 10-fold higher binding affinity but exhibited comparable ERα degradation potency, highlighting the complex pharmacology of ERα.

In 2020, El Ahmad and co-workers performed a medium-throughput screening which led to the development of SAR439859 (Amcenestrant, **12**, Figure 7).[38] SAR439859 induces ERα degradation in MCF-7 cells at subnanomolar

concentrations (ERα degradation IC$_{50}$ = 0.2 nM) with maximal degradation levels of 98% comparable to the *in vitro* activity of Fulvestrant. Medicinal chemistry efforts centered around the phenol moiety, which was replaced with a carboxylic acid in order to lower the log*D* and optimize metabolic stability while maintaining the Glu353/Arg394 hydrogen bond network (Figure 8A). Additionally, expanding the initial cyclohexene ring to

Figure 6. Boronic acid derivatives ZB716 (**10**) and GLL398 (**11**) of Fulvestrant (**5**) and GW7604 (**7**), respectively.

- Lowered logD and improved metabolic stability
- (*S*)-*O*-pyrrolidine best for degradation activity. Open pyrrolidine ring, longer alkyl chain or heterocycles detrimental
- Halogenated aryl groups improved metabolic stability
- Cycloheptene ring provided conformation constraint

12: SAR439859
ERα degradation IC$_{50}$ = 0.2 nM
ERα degradation efficacy = 98%
F = 54% (rat)

Figure 7. SAR summary of SAR439859 (**12**).

Figure 8. X-ray crystal structures of selected SERDs (green carbon atoms) bound to ERα (orange ribbon): SAR439859 **12** (panel A, PBD code 6SBO), LSZ102 **13** (panel B, PDB code 6B0F), AZD9496 **15** (panel C, PDB code 5ACC), GDC-9545 **17** (panel D, PDB code 7MSA) and AZD-9833 **18** (panel E, PDB code 6ZOR). Key hydrogen bonds are represented as dashed lines.

cycloheptene ring provided a slight increase in degradation activity, most likely due to conformational constraint. SAR studies around the aminoethoxy pyrrolidine side chain showed that opening the pyrrolidine ring, increasing the length of the alkyl chain or incorporating other heterocycles was detrimental to degradation activity. Overall, the data suggest that the oxygen and nitrogen atoms of the side chain must be separated by two carbon atoms for optimal degradation efficacy. Regarding the distal phenol moiety, which is associated with high clearance issues, halo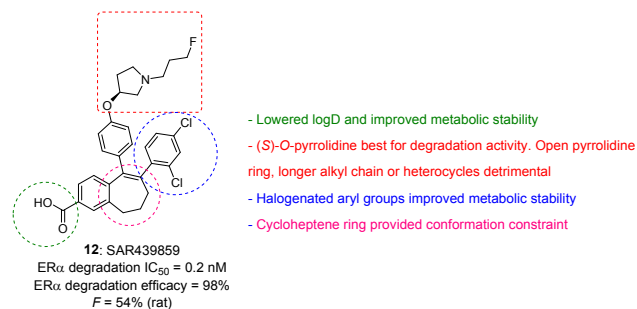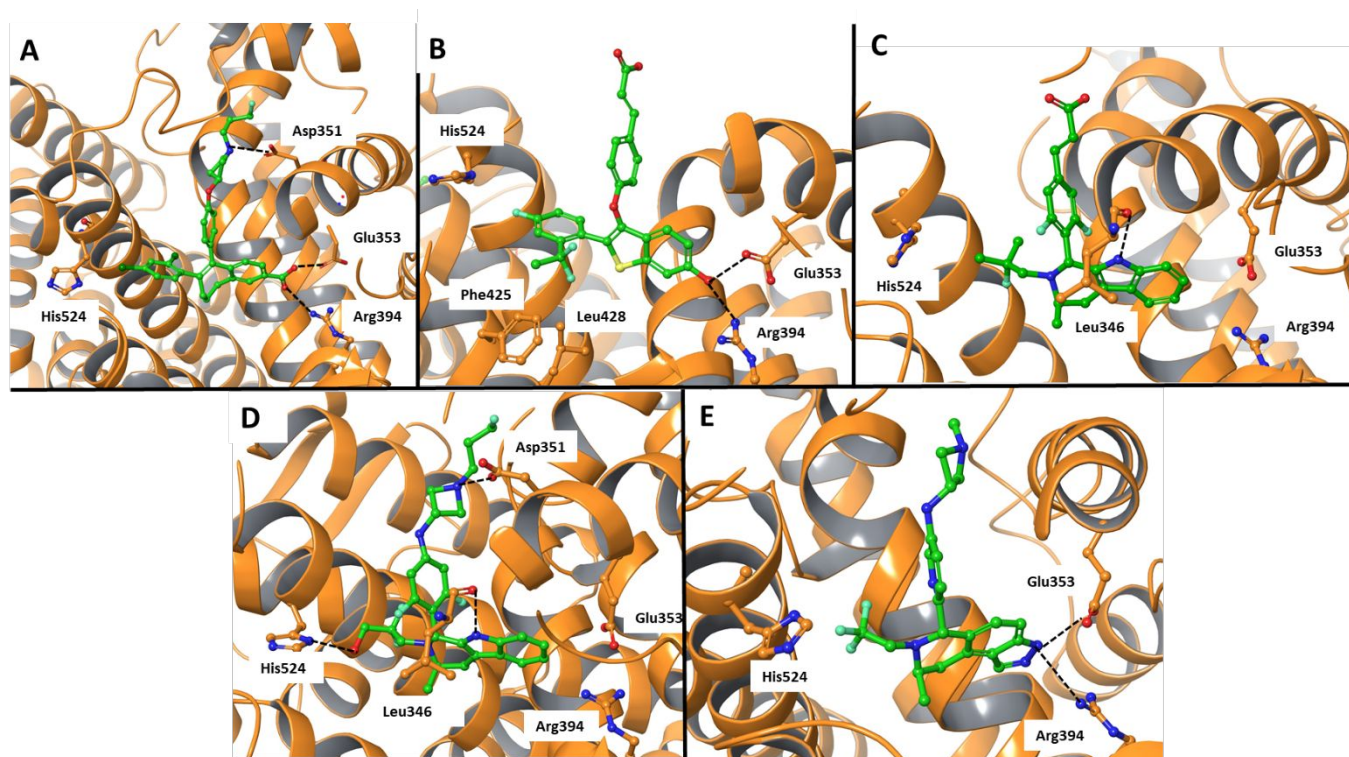genated aryl moieties are required to improve metabolic stability. Interestingly, SAR439859 **12** has one extra methylene group compared with the fluoropropyl azetidine moiety in GDC-9545 (**17**) and AZD9833 (**18**), rendering higher lipophilicity.

3.2. Disruption of planarity

Nonplanar SERMs, such as lasofoxifene **4** (Figure 1), have attenuated phase II metabolism and, consequently, high bioavailability (>60%).[39] Raloxifene has a limited absolute bioavailability of only 2% due to extensive glucurodination at the 6- and 4'-hydroxy positions of the planar benzothiophene (BT) core.[40] Motivated by this rationale, Tria and co-workers introduced substituents at the *ortho* position of the 2-aryl ring and reported the discovery of LSZ102 (**13**, Figure 9) in 2018.[41] The so-called "ortho effect" triggered a torsional constraint which caused the 2-aryl ring to be almost orthogonal to the plane of the BT core. This conformation not only enhances the

pharmacokinetic properties, but it also increases hydrophobic interactions within the ligand binding pocket by occupying a lipophilic pocket near Leu428:Phe425 (Figure 8B). This structural information explained why polar groups are not tolerated in this region of the molecule while *o*-difluoroethyl proved to be optimal for ERα degradation (ERα degradation IC$_{50}$ = 0.2 nM) and antagonism (ERα transcription IC$_{50}$ = 17 nM). Additionally, halogen substituents at the *para* position of the 2-aryl ring further increased bioavailability by blocking phase I hydroxylation metabolic sites.

- Acrylamide tolerated but decreased solubility
- Replacement with pyridine led to slight improvement in ERα degradation efficacy but loss of ERα transcriptional antagonist activity
- *Ortho* group caused 2-aryl ring to be orthogonal to benzothiophene core, minimizing phase II metabolism. *Para* group minimized phase I metabolism

13: LSZ102
ERα degradation IC$_{50}$ = 0.2 nM
ERα degradation efficacy = 83%
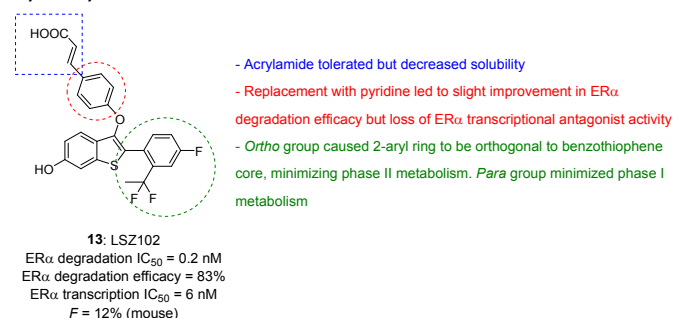ERα transcription IC$_{50}$ = 6 nM
F = 12% (mouse)

Figure 9. SAR summary of LSZ102 (**13**).

3.3. Non-phenolic ERα ligand cores

The phenol ring mimicking the A-ring of estradiol can be replaced with nitrogen-containing heterocycles presenting a suitably oriented N-H hydrogen bond donor for binding. In 2015, Lai and co-workers optimized the triphenylalkene scaffold

of GW7604 (**7**) with the aim to improve exposure following oral dosing. As a result, the authors published an indazole series of SERDs that led to the discovery of GDC-0810 (**14**, Figure 10).[42] In preclinical studies, GDC-0810 displayed robust activity in antagonism (ERα transcription IC_{50} = 2 nM), degradation (ERα degradation EC_{50} = 0.7 nM) and cell viability (MCF-7 antiproliferation IC_{50} = 2.5 nM) assays. However, it behaved as a mixed SERM/SERD and showed partial agonism in uterine models *in vitro* and *in vivo*, in addition to inconsistent ERα downregulation in later reports. Analysis of the SAR studies indicated that the directionality of the indazole N-H was crucial for activity since the corresponding 6-indazole isomer lost > 100-fold ERα degradation potency. Bicyclic heterocycles, including benzothiazalone and benzoxazolone, with weakly acidic N-H groups were able to form weak hydrogen bonds with the canonical Arg391 and Glu353 residues and retained ERα degradation potency. Introduction of methyl or methoxy substituents at the phenyl linker did not lead to an increase in potency while heterocycles (pyridine) led to a 10-fold decrease in ERα degradation potency. Regarding the pendent aryl ring, simultaneous substitution at the *ortho* and *para* positions with halogens provided the most potent analog.
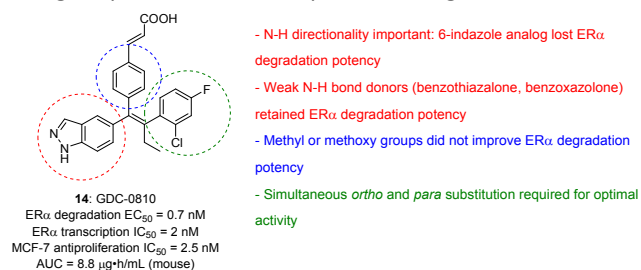

- N-H directionality important: 6-indazole analog lost ERα degradation potency
- Weak N-H bond donors (benzothiazalone, benzoxazolone) retained ERα degradation potency
- Methyl or methoxy groups did not improve ERα degradation potency
- Simultaneous *ortho* and *para* substitution required for optimal activity

14: GDC-0810
ERα degradation EC_{50} = 0.7 nM
ERα transcription IC_{50} = 2 nM
MCF-7 antiproliferation IC_{50} = 2.5 nM
AUC = 8.8 μg•h/mL (mouse)

Figure 10. SAR summary of GDC-0810 (**14**).

In 2015, De Savi and co-workers identified indole derivative AZD9496 (**15**, Figure 11) as a potent ERα degrader (ERα degradation IC_{50} = 0.14 nM) and antiproliferative agent (MCF-7 antiproliferation IC_{50} = 0.04 nM).[43] This compound lacked the common phenolic group for interaction with Arg394 and Glu353 but gained potency through a novel hydrogen bonding interaction between the indole N-H group and the carbonyl of Leu346 (Figure 8C). Furthermore, the chiral methyl substituent provided additional van der Waals interactions within the Phe404:Phe425 lipophilic pocket and the isopropyl fluoro side chain exploited the Leu525:Leu384 lipophilic hole.
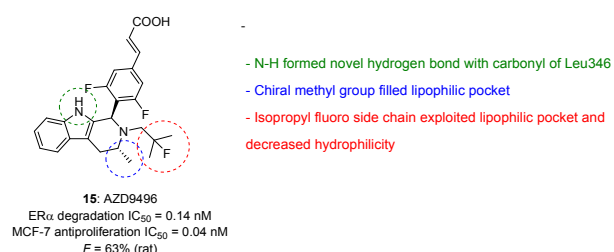

- N-H formed novel hydrogen bond with carbonyl of Leu346
- Chiral methyl group filled lipophilic pocket
- Isopropyl fluoro side chain exploited lipophilic pocket and decreased hydrophilicity

15: AZD9496
ERα degradation IC_{50} = 0.14 nM
MCF-7 antiproliferation IC_{50} = 0.04 nM
F = 63% (rat)

Figure 11. SAR summary of AZD9496 (**15**).

3.4. Basic side chains

Acrylic acid-based oral SERDs (LSZ102 **13**, GDC-0810 **14** AZD9496 **15**) have been discontinued after phase I/II clinical trials due to poor patient tolerability, which could partially be

attributed to the high chemical reactivity derived from the acrylate degradation motif. In this regard, there has been growing interest in switching to basic side-chain SERDs, with the hope of achieving a more promising safety profile. In 2018, Kahraman and co-workers reported the discovery of GDC-0927 (**16**, Figure 12),[44] a chromene-based SERD which was designed to further improve the potency over GDC-0810 (**14**). GDC-0927 exhibited increased *in vitro* potency (ERα degradation IC_{50} = 0.1 nM, ERα degradation efficacy = 97%) and more robust reduction of intratumoral ERα levels. SAR studies focused on optimizing ERα degradation efficacy through side-chain substitution, with azetidine giving the most efficient ERα degrader. Pyrrolidine and piperidine displayed a significant reduction in degradation efficacy. Further extension of the side chain with methyl group was hypothesized to disturb h12 while the terminal fluorine atom minimized phase I metabolism. The development of GDC-0927 (**16**) was discontinued due to low oral exposure and subsequent high pill dosage in clinical trials, which limited dose-escalation studies. A more recent study revealed that the high clearance of GDC-0927 was likely due to the presence of two electron-rich phenols in the molecule.[45] Attempts at replacing the 3'-OH with fluorine, heterocycles, cycloalkyl or alkyl moieties failed to improve the metabolic stability while maintaining potency, reinforcing the requirement for two phenolic groups when it comes to chromene ERα ligands. Had any of these substitutions been successful, they could have expanded the pool of ERα binding motifs to heterocyclic structures lacking the canonical O-N or N-H hydrogen bond donors, thereby inducing a unique ERα conformation and pharmacological profile.
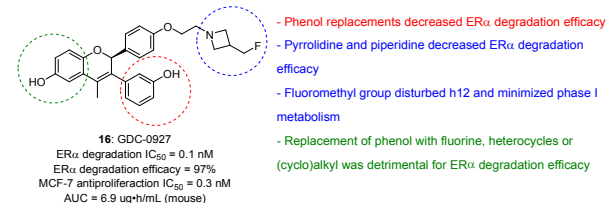

- Phenol replacements decreased ERα degradation efficacy
- Pyrrolidine and piperidine decreased ERα degradation efficacy
- Fluoromethyl group disturbed h12 and minimized phase I metabolism
- Replacement of phenol with fluorine, heterocycles or (cyclo)alkyl was detrimental for ERα degradation efficacy

16: GDC-0927
ERα degradation IC_{50} = 0.1 nM
ERα degradation efficacy = 97%
MCF-7 antiproliferaction IC_{50} = 0.3 nM
AUC = 6.9 ug•h/mL (mouse)

Figure 12. SAR summary of GDC-0927 (**16**).

In 2021, Liang and co-workers published the medicinal chemistry efforts leading to GDC-9545 (Giredestrant, **17**, Figure 13),[46] aiming to address the limitations of GDC-0810 (**14**) and GDC-0927 (**16**). In preclinical studies, GDC-9545 (**17**) displayed potent ERα antagonist activity (ERα transcription IC_{50} = 0.05 nM) and degradation efficacy (ERα degradation efficacy = 101%), which are superior to Fulvestrant and other SERDs in development, including SAR439859 (**12**), AZD-9833 (**18**) and RAD1901 (**19**). GDC-9545 exhibited a full antagonist profile with a reduction in the uterine wet weight and no effect on the endometrium in rat uterine assays. The polar difluoro propyl alcohol chain established a hydrogen bond interaction with His524 (Figure 8D) and significantly attenuated lipophilicity (*c*logP = 5.0) compared with SAR439859 **12** (*c*logP = 9.4) and RAD1901 **19** (*c*logP = 6.8). Additionally, switching the oxygen atom with a nitrogen atom on the basic amino side chain turned out to be critical for optimal antagonism and antiproliferative profile while improving solubility.
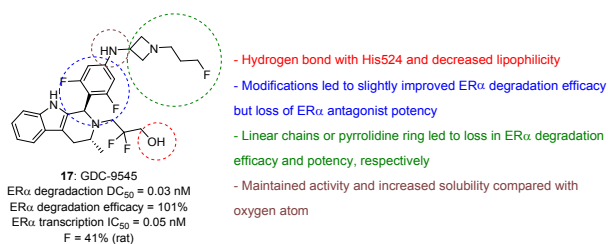
17: GDC-9545
ERα degradaction DC_{50} = 0.03 nM
ERα degradation efficacy = 101%
ERα transcription IC_{50} = 0.05 nM
F = 41% (rat)

- Hydrogen bond with His524 and decreased lipophilicity
- Modifications led to slightly improved ERα degradation efficacy but loss of ERα antagonist potency
- Linear chains or pyrrolidine ring led to loss in ERα degradation efficacy and potency, respectively
- Maintained activity and increased solubility compared with oxygen atom

Figure 13. SAR summary of GDC-9545 (**17**).

Tricyclic indazole AZD-9833 (Camizestrant, **18**, Figure 14) was disclosed in 2020 by Scott and co-workers[47] as a full ERα antagonist and a more potent ERα degrader (ERα degradation IC_{50} = 0.16 nM) than AZD9496 (**15**). AZD9833 and AZD9496 share common structural features, including the chiral methyl group on the piperidine ring and the azetidine side chain, pointing to a shared induced ERα conformation. However, the N-H group of the [5.6.6] indazole core was described to form hydrogen bonds with Arg394 and Glu353 of the ERα binding pocket (Figure 8E), rather than Leu346 as seen in the case of AZD9496 (**15**) and GDC-9545 (**17**). Moreover, the N-H found in this class of SERDs is more basic than the indole N-H of GDC-9545 (**17**), increasing its solubility in aqueous media. Shifting the connectivity of the azetidine ring from an ether was critical to maintain ERα degradation potency and efficacy while lowering lipophilicity. Interestingly, inconsistent ERα degradation across cell lines was observed when the NH linker tether was not directly attached to the azetidine degradation motif. Medicinal chemistry efforts focused on optimizing the different regions of the molecule while modulating logD. To this end, the pyridyl linker and trifluoromethyl terminal group were introduced. The latter not only helped to control the lipophilicity of the resulting compound, but it also modulated the pKa of the neighboring piperidine nitrogen atom.
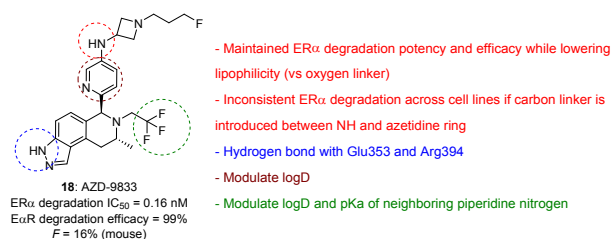

18: AZD-9833
ERα degradation IC_{50} = 0.16 nM
EαR degradation efficacy = 99%
F = 16% (mouse)

- Maintained ERα degradation potency and efficacy while lowering lipophilicity (vs oxygen linker)
- Inconsistent ERα degradation across cell lines if carbon linker is introduced between NH and azetidine ring
- Hydrogen bond with Glu353 and Arg394
- Modulate logD
- Modulate logD and pKa of neighboring piperidine nitrogen

Figure 14. SAR summary of AZD-9833 (**18**).

RAD1901 (Elacestrant, **19**, Figure 15) is a nonsteroidal SERD that displayed a complex U-shaped pharmacology, acting as a weak partial agonist at lower doses and as an antagonist at higher doses.[48] *In vitro* studies showed dose-dependent decrease in ERα levels (ERα degradation IC_{50} = 0.6 nM) and proliferation (MCF-7 antiproliferation IC_{50} = 4.2 nM) comparable to Fulvestrant.[49] RAD1901 has demonstrated potent antitumor activity in multiple patient-derived xenograft models, including some derived from heavily pretreated patients, expressing wild-type or mutant ERα-Y537S and ERα-D538G.

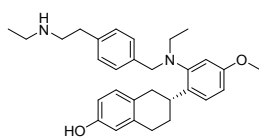**19**: RAD1901

Figure 15. Chemical structure of RAD1901 (**19**).

3.5. Hydrophobic degrons

The repertoire of molecular scaffolds known to induce ERα degradation has been restricted mainly to long perfluoroalkyl chains (as seen in Fulvestrant), the acrylic acid motif found in GW-5638 **6** and basic side chains that exhibit mixed SERM/SERD activity. Expanding the toolbox of degron motifs beyond the above scaffolds is expected to provide new avenues in SERD design. We reported a series of bisphenolic adamantyl ERα ligands attached to structurally novel hydrophobic degrons,[50] among which monocyclic alkanes (**20**, Figure 16) provided antiestrogens having ERα degradation (IC_{50} = 2 nM) and MCF-7 antiproliferation (IC_{50} = 0.5 nM) potencies in the nanomolar range. Our studies suggested that the antiproliferative action of these compounds likely involves distinct contributions from their SERD and ERα antagonism activity.
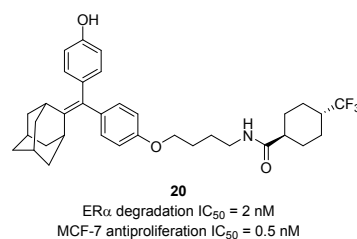

20
ERα degradation IC_{50} = 2 nM
MCF-7 antiproliferation IC_{50} = 0.5 nM

Figure 16. Chemical structure of adamantyl-based SERDs with hydrophobic degrons.

3.6. ERα PROTACs

Proteolysis Targeting Chimeras (PROTACs) have emerged as an attractive addition to the field of drug development thanks to their ability to selectively induce degradation of a protein of interest.[51] These heterobifunctional compounds work in a catalytic fashion, binding simultaneously to an E3 ligase and a target protein. The formation of such a ternary complex facilitates ubiquitin transfer and subsequent proteasomal degradation. This technology has been applied to a wide range of target proteins.[52]

Early ERα PROTAC design consisted of estradiol-based cores linked to short peptidic VHL E3 ligands.[53] In 2019, Hu and co-workers reported a PROTAC (ERD-308, **21**, Figure 17) composed of a raloxifene derivative and a small-molecule VHL ligand.[54] ERD-308 was a highly potent PROTAC (ERα degradation DC_{50} = 0.17 nM and 0.43 nM in MCF-7 and T47D cell lines, respectively) which induced more complete ERα degradation and a stronger antiproliferative effect than Fulvestrant in MCF-7 cells.

Arvinas recently disclosed the structure of their clinical candidate ARV-471 (**22**, Figure 17)[55], which consists of a tetralin core (taken from lasofoxifene **4**) connected to a CRBN E3 ligase recruiter. ARV-471 induced potent ERα degradation in MCF-7 cells (ERα degradation DC_{50} = 1.8 nM) and resulted in superior tumor growth inhibition compared to Fulvestrant in an *ESR1*

mutant patient-derived xenograft model. When combined with the CDK4/6 inhibitor palbociclib, tumor growth inhibition improved to 130%. Initial safety and tolerability reports from ongoing phase I clinical trials showed a favorable safety profile, with no dose-limiting toxicities and no grade 2-4 adverse events observed.
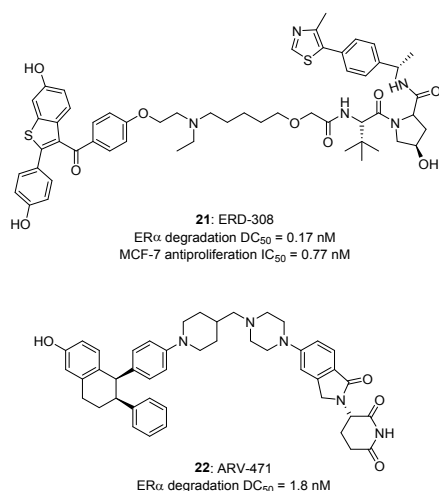

21: ERD-308
ERα degradation DC_{50} = 0.17 nM
MCF-7 antiproliferation IC_{50} = 0.77 nM

22: ARV-471
ERα degradation DC_{50} = 1.8 nM

Figure 17. Chemical structure of ERα PROTACs.

4. Conclusions

Endocrine therapies constitute the therapeutic backbone for the management of ERα-positive breast cancer. The progressive evolution in our understanding of the molecular mechanisms underlying endocrine therapy together with the encouraging clinical efficacy of ERα degraders has sparked interest in the development of potent orally bioavailable SERDs. Recent advances in structural design and optimization of competitive ERα binding, ERα antagonism and ERα degradation in parallel with medicinal chemistry strategies to optimize ADMET properties has led to the prospective development of various clinical candidates. However, a more thorough understanding of the molecular mechanisms by which the different SERDs induce ERα degradation and the link between ERα degradation/antagonism to tumor growth inhibition is necessary to streamline the design of next-generation SERDs. One of the hypotheses driving the development of novel SERDs is that the receptor turnover is one of the best markers for drug efficacy. As a consequence, optimization efforts focus on generating novel SERDs with a degradation efficacy superior to that of Fulvestrant. This assumption may be overlooking other cellular mechanisms, including intranuclear ERα immobilization and impaired ERα mobility,[56] that could be playing a significant role in ERα signalling shutdown. Furthermore, pioneering studies by McDonnel and colleagues suggested that Fulvestrant-mediated ER degradation is not essential for efficacy, but it is likely a marker for full antagonism.[57] Interestingly, McDonnel's recent work also showed the feasibility of using lower and clinically relevant dosages of Fulvestrant (25 mg/Kg) that led to effective tumor inhibition without inducing ER degradation.[58] In another related report, Nettles and colleagues have demonstrated that full antagonism

of ER doesn't require degradation of the receptor.[59] On the other hand, Mader and colleagues showed that suppression of ER-transcription activity by Fulvestrant likely involves SUMOylation of ER.[60] Collectively, these studies highlight several intriguing aspects of the role of degradation and antagonism in SERD-mediated antitumor action. Some other unanswered questions on SERD action involve the gaps in our knowledge of the mechanisms that lead to ubiquitination of ER after binding to a SERD.

Additional challenges arise from the observed suboptimal pharmacokinetic profiles, which translate to high doses during human dose-escalation studies. Modulation of physicochemical properties by introduction of heterocycles (namely pyridine, as in AZD-9833 **18**), fluorine atoms and ether to amine exchange represent the main current trends in this regard. Further structure-based insights, such as exploring new lipophilic pockets, could further address this issue while simultaneously providing a boost in potency. Any possible efficacy advantages will need to be balanced against the emerging safety profile of these agents. One of the other unanswered questions in the clinical setting involves the mechanisms responsible for the low clinical response rate of targeted therapies in endocrine resistant breast cancer. It would be useful to know if this is due to reduced SERD activity in tumor microenvironments or due to posttranslational modification in ER.

Mechanistically, SERDs function via targeted protein degradation (TPD), a therapeutic modality that has recently attracted great attention due to its potential to overcome challenges associated with traditional drug discovery approaches.[61] Targeted protein degradation involves catalytic knockdown of disease-causing proteins which is ultimately expected to confer enhanced efficacy and ability to overcome drug resistance. While Fulvestrant represents one of the first clinically validated targeted protein degradation therapy, the E3 ligase recruited by this SERD remains unknown. More recently, hetero-bifunctional PROTACs that co-opt VHL or Cereblon E3 ligases for ERα degradation have been developed. The human genome is estimated to encode for 600 E3 ligases,[62] but only a handful of these degradation-inducing proteins have been discovered. Identification of new types of E3 ligases and a better understanding of the degradation machinery employed by the currently known SERDs is expected to provide a strong foundation for rational design of antiestrogens capable of overcoming therapy-resistant breast cancer.

Conflicts of interest

There are no conflicts to declare.

Acknowledgements

References

1   R. L. Siegel, K. D. Miller, H. E. Fuchs and A. Jemal, *CA-Cancer J. Clin.* 2022, **72**, 7–33.

2   A. G. Waks and E. P. Winer, *JAMA* 2019, **321**, 288–300.

3   R. Haque, S. A. Ahmed, G. Inzhakova, J. Shi, C. Avila, J. Polikoff, L. Bernstein, S. M. Enger and M. F. Press, *Cancer Epidemiol. Biomarkers Prev.* 2012, **21**, 1848–1855.

4   R. Riemsma, C. A. Forbes, A. Kessels, K. Lykopoulos, M. M. Amonkar, D. W. Rea and J. Kleijnen, *Breast Cancer Res.* Treat. 2010, **123**, 9–24.

5   B. L. Riggs and L. C. Hartmann, *N. Engl. J. Med.* 2003, **348**, 618–629.

6   L. Bergman, M. L. Beelen, M. P. Gallee, H. Hollema, J. Benraadt and F. E. van Leeuwen, *Lancet* 2000, **356**, 881–887.

7   S. R. D. Johnston, *Clin. Cancer Res.* 2001, **7**, 4376s–4387s.

8   J. T. Lei, M. Anurag, S. Haricharan, X. Gou and M. J. Ellis, *Breast* 2019, **48S1**, S26 – S30.

9   A. B. Hanker, D. R. Sudhan and C. L. Arteaga, *Cancer Cell* 2020, **37**, 496–513.

10 J. A. Katzenellenbogen, C. G. Mayne, B. S. Kaztnellenbogen, G. L. Greene and S. Chandarlapaty, *Nat. Rev. Cancer* 2018, **18**, 377–388.

11 D. P. McDonnell, S. E. Wardell and J. D. Norris, *J. Med. Chem.* 2015, **58**, 4883–4887.

12 N. C. Turner, C. Swift, L. Kilburn, C. Fribbens, M. Beaney, I. Garcia-Murillas, A. U. Budzar, J. F. R. Robertston, W. Gradishar, M. Piccart, G. Schiavon, J. M. Bliss, M. Dowsett, S. R. D. Johnston and S. K. Chia, *Clin. Cancer Res.* 2020, **26**, 5172–5177.

13 P. McCormack and F. Spunar, *Clin. Breast Cancer* 2008, **8**, 347–351.

14 J. F. R. Robertson, J. Lindemann J, S. Garnett, E. Anderson, R. I. Nicholson. I. Kruter and J. M. W. Gee, *Clin. Breast Cancer* 2014, **14**, 381–389.

15 M. van Krutchen, E. G. de Vries, A. W. Glaudemans, M. C. van Lanschot, M. van Faassen, I. P. Kema, M. Brown, C. P. Schroder, E. F. de Vries and G. A. Hospers, *Cancer Discov.* 2015, **5**, 72–81.

16 J. F. R. Robertson and M. Harrison, *Br. J. Cancer* 2004, **90**, S7–S10.

17 N. Heldring, A. Pike, S. Andersoon, J. Matthews, G. Cheng, J. Hartman, M. Tujague, A. Ström, E. Treuter, M. Warner and J. A. Gustafsson, *Physiol. Rev.* 2007, **87**, 905–931.

18 A. Farooq, *Curr. Top. Med. Chem.* 2015, **15**, 1372–1384.

19 T. Traboulsi, M. El Ezzy, J. Gleason and S. Mader, *J. Mol. Endocrinol.* 2016, **58**, R15–R31.

20 A. L. Wijayaratne and D. P. McDonnell, *J. Biol. Chem.* 2001, **276**, 35684–35692.

21 A. C. Pike, A. M. Brzozowski, J. Walton, R. E. Hubbard, A. G. Thorsell, Y. L. Li, J. A. Gustafsson and M. Carlquist, *Structure* 2001, **9**, 145–153.

22 Y. L. Wu, X. Yang, Z. Ren, D. P. McDonnell, J. D. Norris, T. M. Willson and G. L. Greene, *Mol. Cell* 2005, **18**, 413–424.

23 X. Puyang, C. Furman, G. Z. Zheng, Z. J. Wu, D. Banka, K. Aithal, S. Agoulnik, D. M. Bolduc, S. Buonamici, B. Caleb, S. Das, S. Eckley, P. Fekkes, M.-H. Hao, A. Hart, R. Houtman, S. Irwin, J. J. Joshi, C. Karr, A. Kim, N. Kumar, P. Kumar, G. Kuznetsov, W. G. Lai, N. Larsen, C. Mackenzie, L.-A. Martin, D. Melchers, A. Moriarty, T.-V. Nguyen, J. Norris, M. O'Shea, S. Pancholi, S. Prajapati, S. Rajagopalan, D. J. Reynolds, V. Rimkunas, N.

Rioux, R. Ribas, A. Siu, S. Sivakumar, V. Subramanian, M. Thomas, F. H. Vaillancourt, J. Wang, S. Wardell, M. J. Wick, S. Yao, L. Yu, M. Warmuth, P. G. Smith, P. Zhu and M. Korpal, *Cancer Discov.* 2018, **8**, 1176–1193.

24 Ciechanover, H. Heller, R. Katz-Etzion and A. Hershko, *PNAS* 1981, **78**, 761–765.

25 Hershko, H. Heller, S. Elias and A. Ciechanover, *J. Biol. Chem.* 1983, **258**, 8206–214.

26 C. M. Pickart and I. A. Rose, *J. Biol. Chem.* 1985, **260**, 1573–1581.

27 E. L. Eckert, A. Mullick, E. A. Rorke and B. S. Katzenellenbogen, *Endocrinology* 1984, **114**, 629–637.

28 M. Fan, A. Park and K. P. Nephew, *Mol. Endocrinol.* 2005, **19**, 2901–2914.

29 N. B. Berry, M. Fan and K. P. Nephew, *Mol. Endocrinol.* 2008, **22**, 1535–1551.

30 P. Totta, V. Pesiri, M. Marino and F. Acconcia, *Plos One* 2014, DOI: 10.1371/journal.pone.0094880.

31 P. Totta, C. Busonero, S. leone, M. Marino and F. Acconcia, *Sci. Rep.* 2016, 23727, DOI: 10.1038/srep23727.

32 S. Kocanova, M. Mazaheri, S. Caze-Subra and K. Bystricky, *BMC Cell Biol.* 2010, **98**, DOI: 10.1186/1471-2121-11-98

33 J. Hoffmann, R. Bohlmann, N. Heinrich, H. Hofmeister, J. Kroll, H. Kuenzer, R. B. Lichtner, Y. Nishino, K. Parczyk, G. Sauer, H. Gieschen, H.-F. Ulbrich, R. Martin and M. R. Schneider, *J. Natl. Cancer Inst.* 2004, **96**, 210–218.

34 T. Yoneya, K. Taniguchi, R. Nakamura, T. Tsunenari, I. Ohizumi, Y. Kanbe, K. Morikawa, S.-I. Kaiho and H. Yamada-Okabe, *Anticancer Res.* 2010, **30**, 873–878.

35 M. Harrison, A. Laight, D. Clarke, P. Giles and R. Yates, *Proc. Am. Assoc. Cancer. Res.* 2003, **22**, 45.

36 L. J. Liu, S. Zheng, V. L. Akerstrom, C. Yuan, Y. Ma, Q. Zhong, C. Zhang, Q. Zhang, S. Guo, P. Ma, E. V. Skripnikova, M. R. Bratton, A. Pannuti, L. Miele, T. E. Wiese and G. Wang, *J. Med. Chem.* 2016, **59**, 8134–8140.

37 K. Liu, S. Zheng, S. Guo, C. Zhang, Q. Zhong, Q. Zhang, P. Ma, E. V. Skripnikova, M. R. Bratton, T. E. Wiese and G. Wang, *ACS Med. Chem. Lett.* 2017, **8**, 102–106.

38 Y. El-Ahmad, M. Tabart, F. Halley, V. Certal, F. Thompson, B. Filoche-Rommé, F. Gruss-Leleu, C. Muller, M. Brollo, L. Fabien, V. Loyau, L. Bertin, P. Richepin, F. Pilorge, P. Desmazeau, C. Girardet, S. Beccari, A. Louboutin, G. Lebourg, J. Le-Roux, C. Terrier, F. Vallée, V. Steier, M. Mathieu, A. Rak, P. Y. Abecassis, P. Vicat, T. Benard, M. Bouaboula, F. Sun, M. Shomali, A. Hebert, M. Levit, H. Cheng, A. Courjaud, C. Ginesty, C. Perrault, C. Garcia-Echeverria, G. McCort and L. Schio, *J. Med. Chem.* 2020, **63**, 512–528.

39 R. L. Rosati, P. Da Silva Jardine, K. O. Cameron, D. D. Thompson, H. Z. Ke, S. M. Toler, T. A. Brown, L. C. Pan, C. F. Ebbinghaus, A. R. Reinhold, N. C. Elliott, B. N. Newhouse, C. M. Tjoa, P. M. Sweetnam, M. J. Cole, M. W. Arriola, J. W. Gauthier, D. T. Crawford, D. F. Nickerson, C. M. Pirie, H. Qi, H. A. Simmons and G. T. Tkalcevic, *J. Med. Chem.* 1998, **41**, 2928–2931.

40 D. Hochner-Celnikier, *Eur. J. Obstet. Gynecol. Reprod. Biol.* 1999, **85**, 23–29.

41 G. S. Tria, T. Abrams, J. Baird, H. E. Burks, B. Firestone, A. Gaither, L. G. Hamann, G. He, C. A. Kirby, S. Kim, F. Lombardo, K. J. Macchi, D. P. McDonnell, Y. Mishina, J. D. Norris, J. Nunez, C. Springer, Y. Sun, N. M. Thomsen, C. Wang, J. Wang, B. Yu, C.-L. Tiong-Yip and S. Peukert, *J. Med. Chem.* 2018, **61**, 2837–2864.

42 A. Lai, M. Kahraman, S. Govek, J. Nagasawa, C. Bonnefous, J. Julien, K. Douglas, J. Sensintaffar, N. Lu, K. J. Lee, A. Aparicio, J. Kaufman, J. Qian, G. Shao, R. Prudente, M. J. Moon, J. D. Joseph, B. Darimont, D. Brigham, K. Grillot, R. Heyman, P. J. Rix, J. H. Hager and N. D. Smith, *J. Med. Chem.* 2015, **58**, 4888–4904.

43 C. De Savi, R. H. Bradbury, A. A. Rabow, R. A. Norman, C. de Almeida, D. M. Andrews, P. Ballard, D. Buttar, R. J. Callis, G. S. Currie, G. J. O. Curwen, C. D. Davies, C. S. Donald, L. J. Feron, H. Gingell, S. C. Glossop, B. R. Hayter, S. Hussain, G. Karoutchi, S. G. Lamont, P. MacFaul, T. A. Moss, S. E. Pearson, M. Tonge, G. E. Walker, H. M. Weir and Z. Wilson, *J. Med. Chem*. 2015, **58**, 8128–8140.

44 S. S. Labadie, J. Li, R. A. Blake, J. H. Chang, S. Goodacrb, S. J. Hartman, W. Liana, J. R. Kiefer, T. Kleinheinz, T. Lac, J. Liao, D. F. Ortwine, V. Mody, N. C. Ray, F. Roussel, M. Vinogradova, S. K. Yeap, B. Zhang, X. Zheng, J. R. Zbieg, J. Liang and X. Wang, *Bioorg. Med. Chem. Lett*. 2019, **29**, 2090–2093.

45 M. Kahraman, S. P. Govek, J. Y. Nagasawa, A. Lai, C. Bonnefous, K. Douglas, J. Sensintaffar, Nhin Liu, K. Lee, A. Aparicio, J. Kaufman, J. Qian, G. Shao, R. Prudente, J. D. Joseph, B. Darimont, D. Brigham, R. Heyman, P.r J. Rix, J. H. Hager and N. D. Smith, *ACS Med. Chem. Lett*. 2019, **10**, 50–55.

46 J. Liang, J. R. Zbieg, R. A. Blake, J. H. Chang, S. Daly, A. G. DiPasquale, L. S. Friedman, T. Gelzleichter, M. Gill, J. M. Giltnane, S. Goodacre, J. Guan, S. J. Hartman, E. R. Ingalla, L. Kategaya, J. R. Kiefer, T. Kleinheinz, S. S. Labadie, T. Lai, J. Li, J. Liao, Z. Liu, V. Mody, N. McLean, C. Metcalfe, M. A. Nannini, J. Oeh, M. G. O'Rourke, D. F. Ortwine, Y. Ran, N. C. Ray, F. Roussel, A. Sambrone, D. Sampath, L. K. Schutt, M. Vinogradova, J. Wai, T. Wang, I. E. Wertz, J.n R. White, S. K. Yeap, A. Young, B. Zhang, X. Zheng, W. Zhou, Y. Zhong and X. Wang, *J. Med. Chem*. 2021, **64**, 11841–11856.

47 J. S. Scott, T. A. Moss, A. Balazs, B. Barlaam, J. Breed, R. J. Carbajo, E. Chiarparin, P. R. J. Davey, O. Delpuech, S. Fawell, D. I. Fisher, S. Gagrica, E. T. Gangl, T. Grebe, R. D. Greenwood, S. Hande, H. Hatoum-Mokdad, K. Herlihy, S. Hughes, T. A. Hunt, H. Huynh, S. L. M. Janbon, T. Johnson, S. Kavanagh, T. Klinowska, M. Lawson, A. S. Lister, S. Marden, D. F. McGinnity, C. J. Morrow, J. Willem, M. Nissink, D. H. O'Donovan, B. Peng, R. Polanski, D. S. Stead, S. Stokes, K. Thakur, S. R. Throner, M. J. Tucker, J. Varnes, H. Wang, D. M. Wilson, D. Wu, Y. Wu, B. Yang and W. Yang, *J. Med. Chem.* 2020, **63**, 14530–14559.

48 F. Garner, M. Shomali, D. Paquin, C. R. Lyttle and G. Hattersley, *Anti-Cancer Drugs* 2015, **26**, 948–956.

49 T. Bihani, H. K. Patel, H. Arlt, N. Tao, H. Jiang, J. L. Brown, D. M. Purandare, G. Hattersley and F. Garner, *Clin. Cancer Res*. 2017, **23**, 4793– 4804.

50 L. Wang, V. S. Guillen, N. Sharma, K. Flessa, J. Min, K. E. Carlson, W. Toy, S. Braqi, B. S. Katzenellenbogen, J. A. Katzenellenbogen, S. Chandarlapaty and A. Sharma, *ACS Med. Chem. Lett*. 2018, **9**, 803–808.

51 M. Békés, D. R. Langley and C. M. Crews, *Nat. Rev. Drug. Discov*. 2022, DOI: 10.1038/s41573-021-00371-6

52 M. Pettersson and C. M. Crews, *Drug Discov. Today Technol*. 2019, **31**, 15–27.

53 K. Cyrus, M. Wekenhel, E.-Y. Choi, H. Swanson and K.-B. Kim, *ChemBioChem*, 2010, **11**, 1531–1534.

54 J. Hu, B. Hu, M. Wang, F. Xu, B. Miao, C.-Y. Yang, M. Wang, Z. Liu, D. F. Hayes, K. Chinnaswamy, J. Delproposto, J. Stuckey and S. Wang, *J. Med. Chem*. 2019, **62**, 1420–1442.

55 L. B. Snyder, presented in part at AACR Annual Meeting, April and May 2021, https://ir.arvinas.com/static-files/7a4db470-3d7f-4d4b-98a4-481b8c573169 (accessed Jan 2022).

56 De Bruyn, J. M. Giltnane, S. J. Hartman, A. Heidersbach, R. Houtman, E. Ingalla, L. Kategaya, T. Kleinheinz, J. Li, S. E. Martin, Z. Modrusan, M. Nannini, J. Oeh, S. Ubhayakar, X. Wang, I.E. Wertz, A. Young, M. Yu, D. Sampath, J. H. Hager, L. S. Friedman, A. Daemen and C. Metcalfe, *Cell* 2019, **178**, 949–963.

57 S. E. Wardell, J. R. Marks, D. P. McDonnell, *Biochem. Pharmacol.* 2011, **82**, 122-130.

58 S E. Wardell, A. P. Yllanes, C. A. Chao, Y. Bae, K. J. Andreano, T. K. Desautels, K. A. Heetderk, J. T. Blitzer, J. D. Norris, D. P. McDonnell, *Breast Cancer Res. Treat.* 2020*,* **179**, 67-77.

59 S. Srinivasan, J. C. Nwachukwu, N. E. Bruno, V. Dharmarajan, D. Goswami, I. Kastrati, S. Novick, J. Nowak, V. Cavett, H.-B. Zhou, N. Boonmuen, Y. Zhao, J. Min, J. Frasor, B. S. Katzenellenbogen, P. R. Griffin, J. A. Katzenellenbogen, K. W. Nettles, *Nat. Chem. Biol.* 2017, **13**, 111-118.

60 T. Traboulsi, M. El Ezzy, V. Dumeaux, E. Audemard, S. Mader, Oncogene, 2019, **38**, 1019-1037.

61 S. B Alabi and C. M. Crews, *J. Biol. Chem.* 2021, **296**, 100647, DOI: 10.1016/j.jbc.2021.100647.

62 P. Jevtić, D. L Haakonsen and M. Rapé, *Cell Chem. Bio*. 2021, **28**, 1000–1013.